Seasonal to inter-annual variability of the Norwegian Atlantic Current: Connection between the northern North Atlantic and the Norwegian Sea

by

Øystein Skagseth

Bjerknes Centre for Climate Research and Geophysical Institute,

University of Bergen, Allegt. 70, 5007 Bergen, Norway.

e-mail: skagseth@gfi.uib.no

tlf: (+47) 55 58 25 96

fax: (+47) 55 58 98 83

First version submitted to Deep-Sea Research (January 2002)

Revised version submitted to Deep-Sea Research (November 2002)

Abstract

Causes for measured variability in the Norwegian Atlantic Slope Current (NwASC) during the period from 1995-2000 are investigated by considering complementary data providing information on the upstream condition and atmospheric forcing. These data are fields of sea surface height (ssh) variability from the TOPEX altimeter, reanalysed mean sea level pressure (mslp), climatological hydrography and repeated hydrographic measurements both in the northern North Atlantic and in the Norwegian Sea. The analysis indicate two different mechanisms associated with different time scales that contribute to the variabilities of the NwASC.

Firstly, for time scales of 2-3 months and 6-12 months, the analyses show significant coherences between the NwASC and the along-stream sea surface slope, and the ssh and the mslp. This can be interpreted as a relation between the wind forcing and NwASC through modulation of the sea surface height. In other words, the variability in the westerly winds modulates the sea surface slope from the northern North Atlantic into the Norwegian Sea, and thus provides a barotropic forcing term for the NwASC. The phase relation from the coherence analysis is such that increased westerly winds occur in phase with an increase of the sea surface slope from the North Atlantic into the Norwegian Sea, and furthermore, this coincides with an increase in the NwASC. The order of this wind effect on the sea level slope is 10^{-7}, and is similar to the basin-scale downward sea surface slope from subtropical to high latitudes in the North Atlantic Ocean. This differential effect on the ssh in the eastern part of the North Atlantic and in the Norwegian Sea can be connected to the variability in the Sverdrup transport. Stronger atmospheric cyclones (westerlies) increase the magnitude of the northward Sverdrup transports in both the northern North Atlantic and in the Norwegian Sea. Combined with the orientation of the isobaths, this lead to increased ssh in the eastern part of the North Atlantic and decreased ssh in the Norwegian Sea.

Secondly, on inter-annual time scales, changes in the hydrographic conditions in the northern North Atlantic coincide with changes in the NwASC. The change in hydrography is also found in the TOPEX ssh data. At inter-annual scales, the ssh in the Iceland Basin (reflecting hydrographic changes) and the NwASC show similar variability. A conceptual mechanism relating the observed anomalies to the NwASC is proposed. Under the assumption of a limited southward extent a cold/warm anomaly in the Iceland Basin would be associated with an anomalously strong/weak eastward geostrophic current to the to south of the anomaly toward the continental slope. Here, the upper (Atlantic) layer becomes thicker, and thus transfers into a northward slope current through conservation of relative vorticity in the upper layer.

Keywords: North Atlantic Current, Norwegian Atlantic Current, sea surface height, sea surface slope, seasonal variability, inter-annual variability

1. Introduction

The aim of this study is to investigate the oceanic coupling between the northern North Atlantic and the Nordic Seas. This is the region of the northernmost path of the Gulf Stream with the North Atlantic Current (NAC) extending into the Norwegian Sea as the Norwegian Atlantic Current (NwAC). The associated fluxes of heat and salt are of major importance in modifying the regional climate. Also the relatively high salinity makes the Atlantic Water (AW) a key ingredient in the transformation to dense intermediate and deep water masses as part of the global thermohaline circulation.

The basic structure of the NAC and its extension into the NwAC is known (Fig. 1). The NAC is divided into two separate northward flowing branches. One branch along the continental slope situated just off the shelf break (e.g. Burrows et al., 1999; Huthnance, 1984) and one branch trough the Iceland Basin (Perkins et al., 1998; Orvik and Niiler, 2001). A two branch system is also observed in the Norwegian Sea: an eastern branch located just off the shelf break hereafter denoted the Norwegian Atlantic Slope Current (NwASC) and a western branch farther offshore as an extension of the Iceland-Faroe frontal jet (Poulain et al., 1996; Orvik et al., 2001). Volume flux estimates of the inflowing Atlantic Water (S>35.0) are about 4.5 Sv for the eastern branch and about 3.5 Sv for the western branch. In terms of fluxes of heat and salt the differences are somewhat larger, because the eastern branch is warmer and saltier than the western branch.

Supposedly the eastern and western branches of the NwAC affect the climate system in the Nordic Seas and the Arctic differently. The western branch provides the interior of the Nordic Seas with more AW which again will have an impact on the regional air-sea exchanges and water mass formation, whereas the eastern branch favours fluxes into the Barents Sea and Arctic. Such arguments provide a link to the reported recent reduction of the Arctic sea ice (e.g. Johannessen et al. 1999; Rothrock, 1999). Thus understanding of the forcing controlling the relative distribution of the eastern and western branches of the NwAC is important in order to understand the climate system within the Nordic and Arctic Seas.

In contrast to the basic structure of the NAC and NwAC which is reasonably well known, quantification of the role of the various forcing mechanisms of this northward flow is lacking. Such knowledge is essential because the type of driving mechanism may provide different constraints on the stability and the variability of the system. This is a very complex issue which certainly depends on the scale under consideration. On time scales from days to weeks the NwASC is closely linked to the wind forcing (Skagseth and Orvik, 2002), whereas the variability of the western branch on such scales is less clear. Also, on seasonal and longer time scales the relative role of the wind and the thermohaline forcing on the variability of the NwASC is not well understood (Hansen and Østerhus, 2000; Orvik et al., 2001).

The focus of this study is on the eastern branch of the NwAC, the NwASC. This branch has been monitored since April 1995 by an array of current meters in the Svinøy section that runs northwestward from the Norwegian coast at 62 ^{o}N and cuts through the two-branch NwAC to the north of the Faroe-Shetland Channel (Fig. 1). Monthly to inter-annual variabilities of the NwASC for the period from 1995 to 2000 are investigated, and causal relationships are sought by considering complementary data of the upstream conditions and forcing. These data are sea surface height (ssh) from the TOPEX altimeter, mean sea level pressure (mslp), monthly climatological hydrography and in addition hydrographic observations, both in the northern North Atlantic and in the Norwegian Sea.

The report is organized as follows: In part 2) observations from the NwASC in the Svinøy section are presented, part 3) contains details from complementary data sets, which are analysed in part 4). Part 5) contains some further analysis and the discussion, and concluding remarks are made in 6).

2. Observations in the Norwegian Atlantic Current

Figure 1 outlines the large-scale surface current pattern of the Atlantic inflow, entering the Norwegian Sea mainly through two pathways - the Faroe-Shetland Channel and over the Iceland-Faroe Ridge. The western branch is an extension of the Atlantic Water running through the Iceland Basin (Perkins et al., 1998), and feeding the Iceland-Faroe Front associated with an eastward running frontal jet (Read and Pollard, 1992). It extends eastward and farther northeastward into the Norwegian Sea as the western branch of the NwAC and tends to follow the topographic slope of the Vøring Plateau (Poulain et al., 1996). The Atlantic inflow through the Faroe-Shetland Channel continues northward along the Norwegian shelf break as the NwASC. This two-branch NwAC was suggested by Poulain et al. (1996) from Lagrangian surface drifter observations. The two-fold structure with a topographically steered slope current and a frontal jet about 200-300 km farther offshore is identified in the Svinøy section by moored and shipboard observations (Orvik et al., 2001).

The hydrographic regime is characterized by the wedge-shaped warm and saline Atlantic Water overlying the fresher and colder intermediate waters (Fig. 2). Orvik et al. (2001) described the annual mean slope current as an along-isobath flow about 40 km wide. The strongest along-slope component of the current is located over the steepest slope between the 200m and 700m isobaths with a maximum of 30cm/s and a decrease relatively uniformly westward to zero at the 1000m isobath. On the deeper side of the current the vertical velocity shear is in accordance with the baroclinic field (Mork and Blindheim, 2000). The tidal currents are small relative to the mean currents in this area, with the major tidal constituent M_2 of the order of 2-3cm/s (Orvik et al., 2001).

Orvik and Skagseth (2002) have shown that the gross variability of the NwASC for periods longer than about 5 days can be represented by a single current meter in the core of the current. Utilizing this result, the low-frequency variability of the NwASC is presented for the period from 1995 to 2000 (Fig. 3) using an Aanderaa Rotating Current Meter (RCM-7) situated at 490 m water depth and instrument depth at 100m in the core of the NwASC. The current data are originally sampled as 1 hour mean values, but in Figure 3 and elsewhere in this article one month mean values of the along slope component is used. The record suggests variability over a broad range of scales but with the seasonal cycle, winter maxima and summer minima, as the most prominent. This holds over the entire record except for the summer and fall of 1995 where the NwASC is anomalously strong relative to the subsequent summer and fall seasons. As a first crude approach seeking causal relationships for the observed variabilities of the NwASC, the NAO-index time series from Jones et al. (1997), essentially reflecting the strength of the westerlies, is also included in Figure 3. The time series suggest that for a range of periods, from monthly to annual scale, the variabilities of the NwASC and the NAO-index tend to co-vary but the correlation coefficient (r) between the series is only 0.36. In particular during the first year (1995-96) the co-variation with the NAO-index is quite different compared to the rest of the period, and the relative NwASC - maximum during the summer of 1995 cannot (at least in a simple manner) be explained by the wind field. In part 4 and 5 a more detailed analysis is performed to investigate the causal relationships between the variabilities in the wind forcing and the NwASC.

3. Complementary data sets

In order to evaluate the observed NwASC variabilities in a broader spatial context, data sets representing the forcing field and ocean state in the Scotland-Iceland region are analysed (Fig. 4).

The atmospheric forcing is expressed by fields of mslp from the Norwegian Meteorological Institute. This data set is originally based on reanalysed mslp data 300 km apart interpolated to fields of 75 km x 75 km spatial resolution at 6 hour time intervals (Reistad and Iden, 1998). The quality of the data has been studied by Jonsson (1991a), and it was found that for periods longer than about 40 hours there was a good agreement between these data and the observed winds at Weather Ship M in the Norwegian Sea, at 66^{o}N, 2^{o}E.

Sea surface height is obtained from the TOPEX altimeter data version WOCE-PODAAC-10d-v2.0. The record covers the period from October 1992 to December 1999. The spatial resolution of the data set is 0.5 deg x 0.5 deg at approximately 10 day time intervals. Corrections applied to the data include wet and dry atmospheric effects, orbit effect, tidal effects and the inverse barometer effect. Also in this data set the mean sea level state at each grid point for the period 1993-1996 is subtracted and hence only information about the ssh variability is contained in the data. Since no tidal model is perfect the tidal correction applied to the ssh is not perfect either. This potential problem of aliasing tides into longer signals has been reduced by the TOPEX satellite repeat period, chosen in order to separate the periods of real oceanic phenomena from the tidal aliasing periods. The TOPEX altimeter aliasing period for the six most energetic tidal components is about 2 months (M_2, S_2, N_2, K_1 and O_1) except for P_1 where it is about 6 months (Schlax and Chelton, 1994). Based on this, special care should be taken when discussing variability in ssh from the TOPEX satellite with time scales of about 2 months.

Monthly fields of temperature and salinity at one degree resolution and standard depths are taken from the World Ocean Atlas - 1998. These data are used to estimate seasonality in steric height in the upper ocean, i.e. basically the contribution upward from the main oceanic thermocline.

Hydrographic variability, both in the northern North Atlantic and in the Norwegian Sea is investigated. In the northern North Atlantic, the hydrographic variability is inferred from repeated XBT sections south of the Iceland-Faroe Ridge in the autumn of 1994, -95, -96 and -97. The data are obtained from the GSDC-IFREMER-Global Subsurface Data Centre. These sections contain temperature information only, but a regionally representative θ-*S* relation is used in steric height estimates.

The hydrographic variability north of the ridge is taken from a repeated profile in a standard section north of the Faroes operated by the Faroese Fisheries Laboratory (data obtained from Bogi Hansen). Here data from 1990 is used in order to cover the TOPEX period. The sampling rate is of the order 3-4 times a year.

4. Analysis of variability

4.1 Sea surface height variability

The TOPEX satellite data is analysed to investigate the ssh variability in the region of the Iceland-Scotland Ridge. Harmonic analysis is applied to retrieve the seasonality in the data (Fig. 5). The estimated amplitudes are larger in the Norwegian Sea than in the North Atlantic, with corresponding phase varying by less than a month. Since the TOPEX data only shows variability from the mean ssh, this means that the slope of the sea surface across the Iceland-Scotland Ridge is at the maximum in March and at the minimum in September. The magnitude of this variability is of the order 10^{-7}, and thus comparable with the basin-scale meridional sea surface slope in the Atlantic Ocean. The explained variance by the ssh annual harmonic of the total ssh variance are in the range from 30-60%, with a tendency for larger values in the eastern part (toward the continental slope) of the investigation area (Fig. 5c).

The estimated annual changes in ssh due to changes in the upper ocean steric height are calculated using monthly fields of temperature and salinity from the World Ocean Atlas - 1998. The annual harmonic explains about 90% of the upper ocean steric height variability for all the investigation area. The estimates are smoother, at least partly due to smoothing/interpolation of the data set onto the 1 by 1 degree grid, but are in general of the same magnitude and phase (Fig. 6 a, b) as the estimated seasonality from the TOPEX ssh data (compare with Fig. 5 a, b). The largest discrepancy between these results is found in the northeastern part of the study area (about 63-64^{o}N, 5^{o}W-2^{o}E) where the estimated amplitudes based on the TOPEX ssh data exceed those based on hydrography.

To further analyse the spatial and temporal variability of the ssh, an Empirical Orthogonal Function (EOF) analysis is performed. Prior to this analysis, the contribution due to the annual change in upper ocean steric height (Fig. 6) is removed from the ssh data. Alternatively, the annual cycle of the ssh data could have been filtered out. However this would also have removed annual scale contributions to the ssh that are not related to the upper ocean steric change, and therefore this method is not used.The data are also smoothed in time using a moving-average filter with a one month cut-off period.

The two leading EOF modes capture 49.5% and 11.8% of the variance, and are statistically significant. One should note that these magnitudes depend on the size of the investigation area and the time filtering applied to the data prior to the analysis.

EOF mode 1 shows the highest magnitudes in the Norwegian Sea. The unipole pattern means that variabilities due to this mode are in phase in the northern North Atlantic and in the Norwegian Sea (Fig. 7a). The principal component indicates variability over a broad range of scales from months to inter-annual (Fig. 7b). Also noteworthy are two longer-periodic trends through 1993-1995 and 1996-1999, separated by a “jump” in 1995.

EOF mode 2 describes a dipole pattern with a nodal line over the Iceland-Faroe Ridge, turning north-eastward into the Norwegian Sea (Fig. 7c). The dipole EOF pattern means that the ssh varies in opposite phase across the nodal line, i.e. essentially across the Iceland-Faroe Ridge. The associated principal component shows that this pattern essentially contain seasonal variability with varying amplitude through the record (Fig. 7d).

4.2 The mean sea level pressure data

The mslp variability in the study region is retrieved by EOF analysis. Prior to the analysis the mean value at each grid point is removed and the data are smoothed in time using a moving average filter with a one month cut-off period in a similar manner to the ssh data (section 4.1). Here only the leading EOF mode, capturing 76.5% of the variance, is discussed. This mode contains a unipole pattern with centre of action just south-east of Iceland (Fig. 8a). Combined with its principal component (Fig. 8b) this mode basically represents a measure of the average strength of the atmospheric lows (cyclones), and also the strength of the westerlies, with winter maxima and summer minima. Striking features are the “state-switch” in 1995- 1996, and the apparent long-period trends with growing amplitudes in 1992-1995 and 1996-1999.

4.3 Hydrography

The hydrographic variability both in the northern North Atlantic and within the Norwegian Sea are investigated. The changes are estimated in terms of steric height variability for comparability with the ssh variability from the TOPEX altimeter. The steric height variability is estimated from 700m depth to the surface, relative to a reference water mass with S=35 and $\theta=0^{o}C$.

In the northern North Atlantic the hydrographic variability is taken from four repeated sections in the subsequent autumn seasons from 1994 to 1997 south of the Iceland-Faroe Ridge, through the Iceland Basin (Fig. 4). The sections contain only temperature, and thus estimation the effect on the steric height variability requires some assumptions about the salinity. By considering the annual mean θ-S profile near the centre of the section at 62^{o}N, 13^{o}W a nearly linear relation is found between 700 and 50 m, with correlation coefficient $r > 0.99$. Thus, under the assumption that salt and temperature anomalies vary in phase, the salinity can be approximated by the linear relation $S=0.059*\theta+34.77$, in the estimates of steric height estimates changes. The temporal evolution of the steric height variability shows a negative anomaly in the section for the years 1994 and 1995 of < -2cm, and a transition toward a positive anomaly of > 2cm in 1997 (Fig. 9). The changes are in accordance with the observed warming of the upper ocean from 1994-95 to 1996-97 in the sections through the Iceland Basin (not shown).

The hydrographic variability within the Norwegian Sea is represented by a repeated vertical profile north of the Faroes at 64^{o}00’N and 6^{o}05’W. This profile is situated on the cold side of the Iceland-Faroe Front outside the region of seasonal frontal displacement reported by Hansen et al. (2000). The steric height variability shows a marked seasonal cycle, with an amplitude of the order of 2cm (Fig. 10). In the time period of the TOPEX satellite, the most pronounced anomaly relative to the annual harmonic is the transition from weak but positive values in summer of 1996 to negative values in the two following years, i.e. a dense (cold) anomaly.

5. Discussion

Based on direct observations of the variabilities in the NwASC, the ssh, hydrography and the wind field (mslp), it is tempting to investigate the mechanism of their coupling.

In particular, with the TOPEX ssh fields, relations between variabilities in the NwASC and in the ssh are of interest. Assuming the NwASC has the properties of a local geostrophically balanced flow, the sea surface slope mirrors the bathymetry, i.e. the sea surface slopes downward from the shelf toward deeper water, and reflects the current speed. Assuming dx=40km for example, an uncertainty in $d\zeta$ of +/-2cm gives an uncertainty range of the order of 10cm/s through the geostrophic relation: $fv = g\, d\zeta/dx$. The accuracy of the TOPEX satellite altimeter data of about +/- 2 cm is thus insufficient to properly resolve the variability of this narrow flow.

Covariations between ocean currents and sea level slope have been discussed for the Atlantic and Pacific coast of the United States (Sturges, 1974). Huthnance (1984) showed a linear relation between the along-slope current and the along stream sea surface slope (sss) through the Joint Effect of Baroclinicity and Relief (JEBAR). However much of the variabilities focused herein are on shorter time scales than those associated with JEBAR variability of a year or more. The annual scale variability due to JEBAR is probably small in the region of the northern North Atlantic and the Norwegian Seas, indicated by the similar amplitudes and phases of the annual upper ocean steric change across the Iceland-Scotland Ridge (Fig. 6). Also the rather broad range of observed variabilities in the NwASC including relatively short time scales of months (Fig. 3) indicate a barotropic forcing mechanism.

To investigate whether relations between ssh and, strength of the NwASC find support in observations coherence analyses between the NwASC and sea level slopes in along- and cross-stream direction are performed. In the along-stream direction the sss both in the eastern: (ssh(A)-ssh(B))/$\Delta X_{A\text{-}B}$ and the western: (ssh(C)-ssh(D))/$\Delta X_{C\text{-}D}$ part of the study area (areas shown in

Fig. 4) are significantly coherent with the NwASC for periods of about 3 and 6-12 months (Fig. 11 a, c). Note that the shortest resolved period in this analysis is 2 months. The phase relation is similar for these records (Fig. 11 b, d), with the sss index leading the NwASC for the periods of about 3 months with $\pi/4$, i.e. about 11 days. For the 6-12 month periods there is a tendency for positive phase, meaning the NwASC leads the sss but this is not significant. However, this is probably an artifact, due to the combined effect of contributions from the remaining annual steric signal in the sss (the mean annual steric cycle was removed prior to this analysis) and the wind forcing, that are out of phase. The cross-flow sss in the North Atlantic: (ssh(A)-ssh(C))/ $\Delta X_{A\text{-}C}$ is not significantly coherent with the NwASC, except for the longest resolved period (2 years). The cross-flow sss in the Norwegian Sea: (ssh(B)-ssh(D))/$\Delta X_{B\text{-}D}$ shows peaks in the coherence spectrum for similar periods to the along slope flow but these peaks are less significant. The phase relation between these series is inconclusive due to large errors. It should be noted that in this analysis, only data points without gaps are included. The error and tendency for missing data for TOPEX altimeter data is generally larger on the shelves and on steeper part of the continental slopes. Thus the ssh data included in this study are possibly not optimal for resolving the cross-flow sss associated with the NwASC.

With the statistically significant relation between the along-stream sss and the NwASC from the coherence analysis (Fig. 11 a-d) we proceed by investigating the cause for this sea level change. This is performed by analysing the coherence (Fig. 12) between the principal components associated with the leading satellite ssh modes (Fig. 7 b,c) and the leading mslp mode (Fig. 8b). The normalized principal components of the SSH-PC1 and MSLP-PC1 is shown in Figure 12a. These series show a very broad peak in the coherency estimates (Fig. 12 c-d). For periods of about 3-4 months and longer the coherency estimates mostly exceed that of the 90% significance level. The corresponding phase between these series show a small lag for the SSH-PC1 relative to the MSLP-PC1 but this is not significant at the 90% level. The interpretation of this, when also considering the spatial pattern associated with these principal components, is that stronger/weaker atmospheric cyclones (and westerly winds) increase/decrease the sea surface slope from the North Atlantic into the Norwegian Sea.

The normalized principal components of the SSH-PC2 and MSLP-PC1 are shown in Figure 12b. The coherence spectrum between these series show a significant peak for periods of 8-12 months that is about -140^{o} out of phase (Fig. 12 e-f). The dipole pattern of the SSH EOF2 (Fig. 7b) means that the variabilities in the ssh in the North Atlantic and in the Norwegian Sea due to this mode are in opposite phase. Combined with the principal components this means stronger/ weaker atmospheric cyclones (and westerly winds) increase/decrease the sea surface height in the northern North Atlantic whereas the opposite effect is found in the Norwegian Sea. Thus the combined effect of the SSH-PC2 and MSLP-PC1 include a steepening of the sea surface slope from the North Atlantic into the Norwegian Sea with increasing westerly winds. This differential effect on the ssh in the eastern part of the North Atlantic and in the Norwegian Sea can be connected to the variability in the Sverdrup transport. The spatial pattern of the leading mslp eof mode, basically representing the anomalous strength of the atmospheric cyclone, provide a link to variability in the northward Sverdrup transport:

$$M^{\varphi} = \frac{1}{\beta}\underline{k} \cdot (\nabla \times \tau)$$

where $\beta = \frac{\partial f}{r\partial\phi}$, f is the Coriolis parameter, r is the radius of the earth, ϕ is the latitude and τ the wind stress. Thus anomalous stronger/weaker cyclones lead to anomalous increase/decrease in the northward Sverdrup transport. The associated zonal transport, integrated from the eastern boundary to the interior, yields:

$$M^{\lambda} = \frac{1}{r}\int_{\lambda_{interior}}^{\lambda_{east}} \frac{\partial M^{\varphi}}{\partial\phi} d\lambda$$

where λ is the longitude. Based on observed wind stress data Veronis (1973) found annual mean northeasterly Sverdrup transport in the eastern part of the North Atlantic, i.e. toward the eastern continental slope and the Iceland-Scotland Ridge. The variability in the wind forcing contained in the leading mslp eof mode represents the variability of the regional north-eastward Sverdrup transport. In the southern part of the Norwegian Sea the Sverdup transport is basically north-eastward (Jonsson, 1991b). A possible mechanism is therefore that stronger atmospheric cy-clones (westerlies) increase the magnitudes of the Sverdrup transports in both the northern North Atlantic and in the Norwegian Sea, but that combined with the orientation of the isobaths this lead to increased ssh in the eastern part of the North Atlantic and decreased ssh in the Nor-wegian Sea.

The relations obtained between variabilities in the NwASC and the sea surface slopes, and the leading modes of the ssh and the mslp, have an important implication with respect to the driving force of the NwASC. The results presented herein suggest a relation between the wind forcing and the NwASC through modulation of the sea surface height. The variability in the wind forc-ing modulates the sea surface slope from the northern North Atlantic into the Norwegian Sea, and thus provides a barotropic forcing term for the NwASC. The phase relation is such that, in general, increased westerly winds increase the sea surface slope from the North Atlantic into the Norwegian Sea, and lead to an increase of the NwASC. The magnitude of this variability is of a similar order to the generally downward sea surface slope from equatorial to high latitudes in the Atlantic of, 10^{-7}.

In addition to the variability at relatively short time scales previously discussed, the different data sets also contain variabilities at inter-annual time scales. In particular, the hydrographic condition in the Iceland Basin between 1995 and 1996, based on the repeated XBT sections (see Fig. 9), show substantial changes. These changes are in accordance with observations further to the south, where an overall increase of the temperature and thickness, and decrease of the density, of the Subpolar Mode Water, accompanied by an increase of its salinity east of the Reykjanes Ridge, was reported from 1995 to 1996 (Bersch et al., 1996). This change in hydrography coincides with the record high change in the winter NAO index between subsequent years, from a positive state in 1994-95 to a negative state in 1995-96 (Jones et al., 1997).

These anomalies found in the repeated XBT and CTD sections in the North Atlantic are also observed in the TOPEX ssh data. Both of the two leading ssh EOF modes contribute to an increase in the ssh from 1995 to 1996 in the North Atlantic, whereas in the Norwegian Sea their combined effects tend to cancel out. This suggests that changes in the westerlies have a larger impact on hydrography in the North Atlantic as compared to the Norwegian Sea, under the assumption that the variabilities in the westerlies are the primer for the change from 1995 to 1996. Further investigates of the covariance between hydrographic changes in the North Atlantic and changes in the Atlantic Inflow normalized time series representing the variabilities of the NwASC and the ssh in the Iceland Basin (area C in Fig. 4), are shown in Figure 13. In both these records the annual cycle is the most prominent signal (Fig. 13a). Longer time scale variability is indicated in the series with maxima in the series in 1995, minima in 1996-97, and increasing values until 1999 (Fig. 13b). The correlation coefficients (r) are 0.62 when the annual cycle is included (Fig. 13a), and 0.53 when the annual signal is removed (Fig. 13b).

Independent of origin, some general remarks can be made about the effect of hydrographic anomalies on the NwASC. Since cold/warm anomalies in the Iceland Basin are associated with anomalously dense/light water, this again would affect the density field, and thus also the circulation. Under the assumption of a limited southward extent, the cold anomaly in 1994-95 would be associated with an anomalously high eastward geostrophic current to the to south of the anomaly toward the continental slope. Here, the upper (Atlantic) layer becomes thicker (see e.g. http://sam.ucsd.edu/vertical_sections/Atlantic.html) and thus transfers into a northward slope current through conservation of relative vorticity in the upper layer ($\eta^{(u)}/H^{(u)}$=const, where $\eta^{(u)}$

and $H^{(u)}$ are respectively the relative vorticity and the thickness of the upper layer). Such argumentation provides a direct link between cold (dense) anomalies in the northern North Atlantic (mainly in the Iceland Basin) as observed in 1994-95 and the observed anomalously strong NwASC during 1995. Similar but opposite argumentation would work for warm (light) anomalies.

6. Concluding remarks

Variabilities in the NwASC during the period from 1995-2000 are investigated by considering complementary data providing information on the upstream and atmospheric forcing. Time scales from a few months up to inter-annual scales have been considered. The analysis indicates two different mechanisms associated with different time scales that contribute to the variabilities of the NwASC.

Firstly, for time scales of 2-3 months and 6-12 months, the analysis shows a significant coherence between the NwASC and the along-stream sea surface slope, and the ssh and the mslp. This can be interpreted as a relation between the wind forcing and NwASC through modulation of the sea surface height. In other words, the variability in the westerly winds modulates the sea surface slope from the northern North Atlantic into the Norwegian Sea, and thus provides a barotropic forcing term for the NwASC. The phase relation from the coherence analysis is such that increased westerly winds occur in phase with an increase of the sea surface slope from the North Atlantic into the Norwegian Sea, and furthermore, this coincides with an increase in the NwASC. The order of this wind effect on the sea level slope is 10^{-7}, and is similar to the basin-scale downward sea surface slope from sub-tropical to high latitudes in the North Atlantic Ocean. This differential effect on the ssh in the eastern part of the North Atlantic and in the Norwegian Sea can be connected to the variability in the Sverdrup transport.

Stronger atmospheric cyclones (westerlies) increase the magnitudes of the Sverdrup transports in both the northern North Atlantic and in the Norwegian Sea. Combined with orientation of the isobaths, this lead to increased ssh in the eastern part of the North Atlantic and decreased ssh in the Norwegian Sea.

Secondly, on inter-annual time scales, changes in the hydrographic conditions in the northern North Atlantic coincide with changes in the NwASC. The change in hydrography is also found in the TOPEX ssh data. The ssh in the Iceland Basin (reflecting hydrographic changes) and the NwASC show similar variability. A conceptual mechanism relating the observed anomalies to the NwASC is proposed. Under the assumption of a limited southward extent, a cold/warm anomaly in the Iceland Basin would be associated with an anomalous strong/weak eastward geostrophic current to the to south of the anomaly toward the continental slope. Here, the upper (Atlantic) layer becomes thicker, and thus transfers into a northward slope current through conservation of relative vorticity in the upper layer.

References

Bersch, M., Meincke, J., Sy, A. (1999) Interannual thermohaline changes in the northern North Atlantic 1991-1996. Deep-Sea Research II, 46, 55-75.

Burrows, M., Thorpe, S.A., Meldrum, D.T. (1999) Dispersion over the Hebridean and Shetland shelves and slopes. Continental Shelf Research, 19, 49-55.

Hansen, B., Østerhus, S. (2000) North Atlantic - Nordic Seas exchanges. Progress in Oceanography 45, 109-208.

Huthnance, J.M. (1984) Slope currents and “JEBAR”. Journal of Physical Oceanography, Vol. 14, 795-810.

Johannessen, O.M., Shalina, E.V., Miles, M.W. (1999) Satellite evidence for an arctic sea ice cover in transformation. Science, 286, 1937-1939.

Jones, P.D., Jonsson, T., Wheeler, D. (1997) Extension to the North Atlantic Oscillation using early instrumental pressure observations from Gibraltar and South-West Iceland. International Journal of Climatology, 17, 1433-1450.

Jonsson, S. (1991a) A comparison between wind stresses, based on geostrophically derived and observed winds, at Weather Ship M in the Norwegian Sea. Deep-Sea Research, 38, 607-615.

Jonsson, S. (1991b) Seasonal to interannual variability of wind stress curl over the Nordic Seas. Journal of Geophysical Research, 96, C2, 2649-2659.

Mork, K.A., Blindheim, J. (2000) Variations in the Atlantic inflow to the Nordic Seas, 1955-1996. Deep-Sea Research I 47, 1035-1057.

Orvik, K.A., Niiler, P. (2002) Major pathways of Atlantic water in the northern North Atlantic and Nordic Seas toward the Arctic. Geophysical Research Letters, in press.

Orvik, K.A, Skagseth, Ø. (2002) Monitoring the Norwegian Atlantic Slope Current using a single moored current meter. Continental Shelf Research, in press.

Orvik, K.A., Skagseth, Ø., Mork, M. (2001) Atlantic Inflow to the nordic seas: current structure and volume fluxes from moored current meters, VM-ADCP and SeaSoar-CTD observations, 1995-1999, Deep-Sea Research I 48, 937-957.

Perkins, H., Hopkins, T.S., Malmberg, S.A., Poulain, P.M., Warn-Varnas, A. (1998) Oceanographic conditions east of Iceland. Journal of Geophysical Research, 103, 21531-21542.

Poulain, P.-M., Warn-Varnas, A., Niiler, P.P. (1996) Near-surface circulation of the Nordic seas as measured by Lagrangian drifters. Journal of Geophysical Research, 101, C8, 18237-18258.

Read, J.F., Pollard, R.T. (1992) Water masses in the region of the Iceland-Faeroes Front. Journal of Physical Oceanography, 22, 1365-1378.

Reistad, M., Iden, K. (1998) Updating, correction and evaluation of the hindcast data base of air pressure, wind and waves for the North Sea, The Norwegian Sea and the Barents Sea. Res. Rep. No. 9, The Norwegian Meteorological Institute. 42 pp.

Rothrock, D.A., Yu, Y., Maykut, G.A. (1999) Thinning of the Arctic sea ice cover. Geophysical Research Letters, 26, 3469-3472.

Schlax, M. G., Chelton, D.B. (1994) Aliased tidal errors in TOPEX/POSEIDON sea surface height data. Journal of Geophysical Research, 99, C12, 24761-24775.

Skagseth, Ø., Orvik., K.A. (2002) Identifying fluctuations in the Norwegian Atlantic Slope Current by means of Empirical Orthogonal Functions. Continental Shelf Research, 22, 547-563.

Sturges, W. (1974) Sea level slope along continental boundaries. Journal of Geophysical Research, 79, 6, 825-830.

Veronis, G. (1973) Model of the World ocean Circulation: I. Wind-driven, two layer. Journal of Marine Research, 229-289.

Acknowledgement

The author is grateful to Martin Mork, Kjell A. Orvik, Knut Barthel, Peter M. Haugan and Alastai Jenkins for constructive interest in the phase of putting these ideas on paper and for many valuable suggestions helpful in order to improve the manuscript. Hydrographic data north of the Faroes were kindly provided by Bogi Hansen of the Faroese Fisheries Laboratory. The work has received financial support from the Norwegian Research Council programme NO-CLIM.

Figure text

Figure 1. Schematic of the major pathways of Atlantic water (grey lines) in the investigation area. The Svinøy Section is shown (thin black line) starting at about 62^{o}N and going toward the northwest. Contoured isobaths are 2, 5, 10, 20, 30 and 40 hectometre.

Figure 2. Hydrography in the Svinøy Section showing a) potential temperature, b) salinity and c) potential density. The current meter record considered in this study is obtained over the 490m isobath at 100m instrument depth (●).

Figure 3. Along-slope component of velocity in the NwASC based on current meters in the Svinøy section (solid line) and NAO index (dashed line). One month averaged values. The correlation coefficient (r) between the series is 0.36.

Figure 4. Map of the investigation area showing data used in this study: (●) indicates altimeter points, XBT section in the northern North Atlantic, and CTD profile north of the Faroes. The defined boxes A-D are used to estimate the sea surface slopes discussed in Figure 11.

Figure 5 a-c. Calculated sea surface height annual cycle based on the TOPEX altimeter data showing a) amplitude in cm, b) phase in months and c) the amount of variance explained by the annual harmonic in percent.

Figure 6 a-b. Calculated steric contribution to the annual cycle sea surface height for the upper 700m including a) amplitude in cm and b) phase in months. Estimates are based on the World Ocean Atlas - 1998 data set.

Figure 7 a-d. EOF analysis of the TOPEX ssh data showing a) the first EOF mode and b) its associated principal component, c) the second EOF mode and b) its associated principal component. Previous to plotting the EOF patterns are multiplied with the standard deviation of their associated principal component, and the principal components are divided by their associated standard deviations. The unit is in cm. One month low-pass filtered data.

Figure 8 a-b. a)The leading EOF mode of Hindcast mslp data and b) the associated principal component. Previous to plotting the EOF pattern is multiplied with the standard deviation of the associated principal component, and the principal component is divided by the associated standard deviation. The unit is in mbar. One month low-pass filtered data.

Figure 9. Steric height anomaly based on an XBT temperature section between Scotland and Iceland. The XBT section is shown in figure 4.

Figure 10. Steric height anomaly based on a CTD station north of the Faeroes at $64^{o}00'$N, $6^{o}05'$W (see figure 4), including the estimate based on the individual profiles (*) and the associated annual harmonic (- -).

Figure 11 a-h. Coherence analysis between the NwASC and various sea level slopes defined as a-b) ssh(A) - ssh(B) , c-d) ssh(C) - ssh(D) , e-f) ssh(A) - ssh(C) and g-h) ssh(B) - ssh(D). The areas A-D are shown in Figure 4. The lower and upper dashed lines in the coherence squared estimates indicate the 95% and 99% significance levels. In the phase plot the dashed lines indicate the 95% significance interval. One month low-pass filtered data.

Figure 12 a-f. Principal component time series of a) SSH-PC1 (thin line) and MSLP-PC1 (thick line) and b) SSH-PC2 (thin line) and MSLP-PC1 (thick line). Coherence analysis between the series c-d) SSH-PC1 and MSLP-PC1 e-f) SSH-PC2 and MSLP-PC1. The lower/upper dashed lines in the coherence squared estimates indicate the 95/99% significance levels. In the phase plot the dashed lines indicate the 95% significance interval. One month low-pass filtered data.

Figure 13 a-b. a) Normalized time series of TOPEX ssh in box C (box shown in Figure 4) and the NwASC and b) similar but with the seasonal signal removed. Note that the ssh variability is multiplied by -1 for comparison with the NwASC. The mean contribution of the annual steric height change to ssh (shown Figure 6) is removed for the TOPEX ssh data prior to the analysis. One month low-pass filtered data.

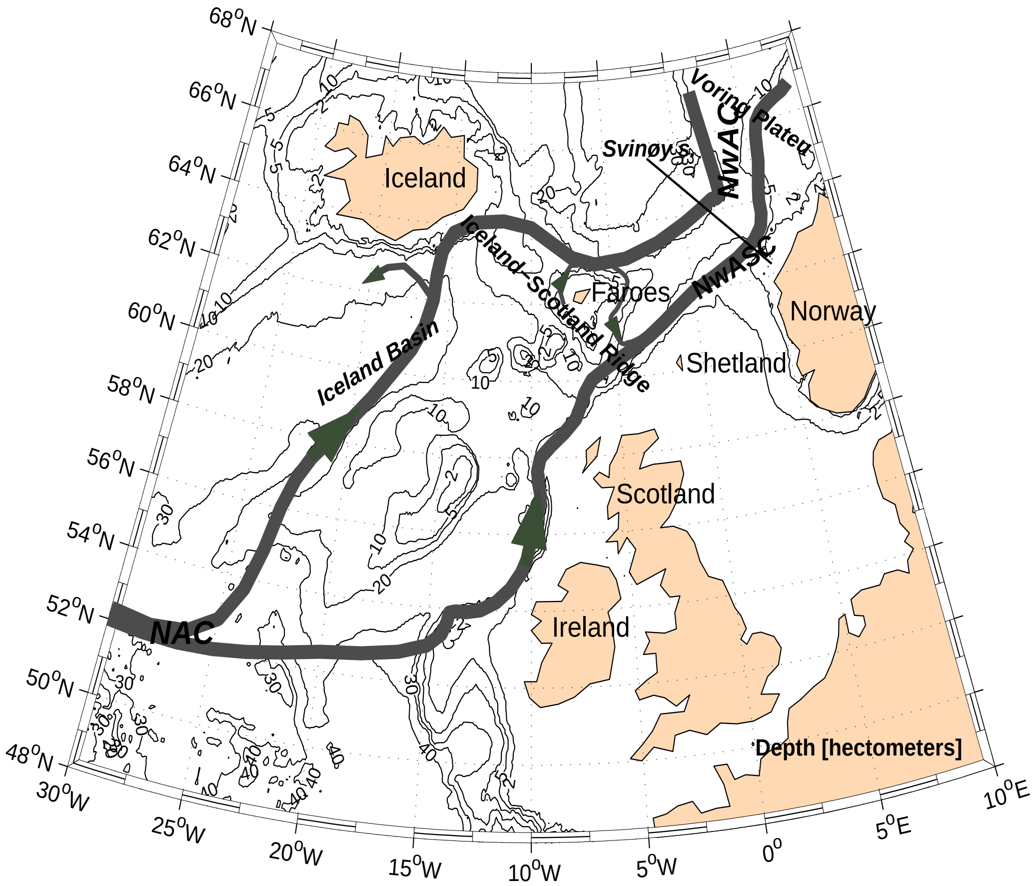
Iceland
Faroes
Norway
Shetland
Scotland
Ireland
Iceland Basin
Iceland–Scotland Ridge
Voring Plateu
Svinøy S.
NwAC
NwASC
NAC
Depth [hectometers]
68°N
66°N
64°N
62°N
60°N
58°N
56°N
54°N
52°N
50°N
48°N
30°W
25°W
20°W
15°W
10°W
5°W
0°
5°E
10°E

Figure 1.

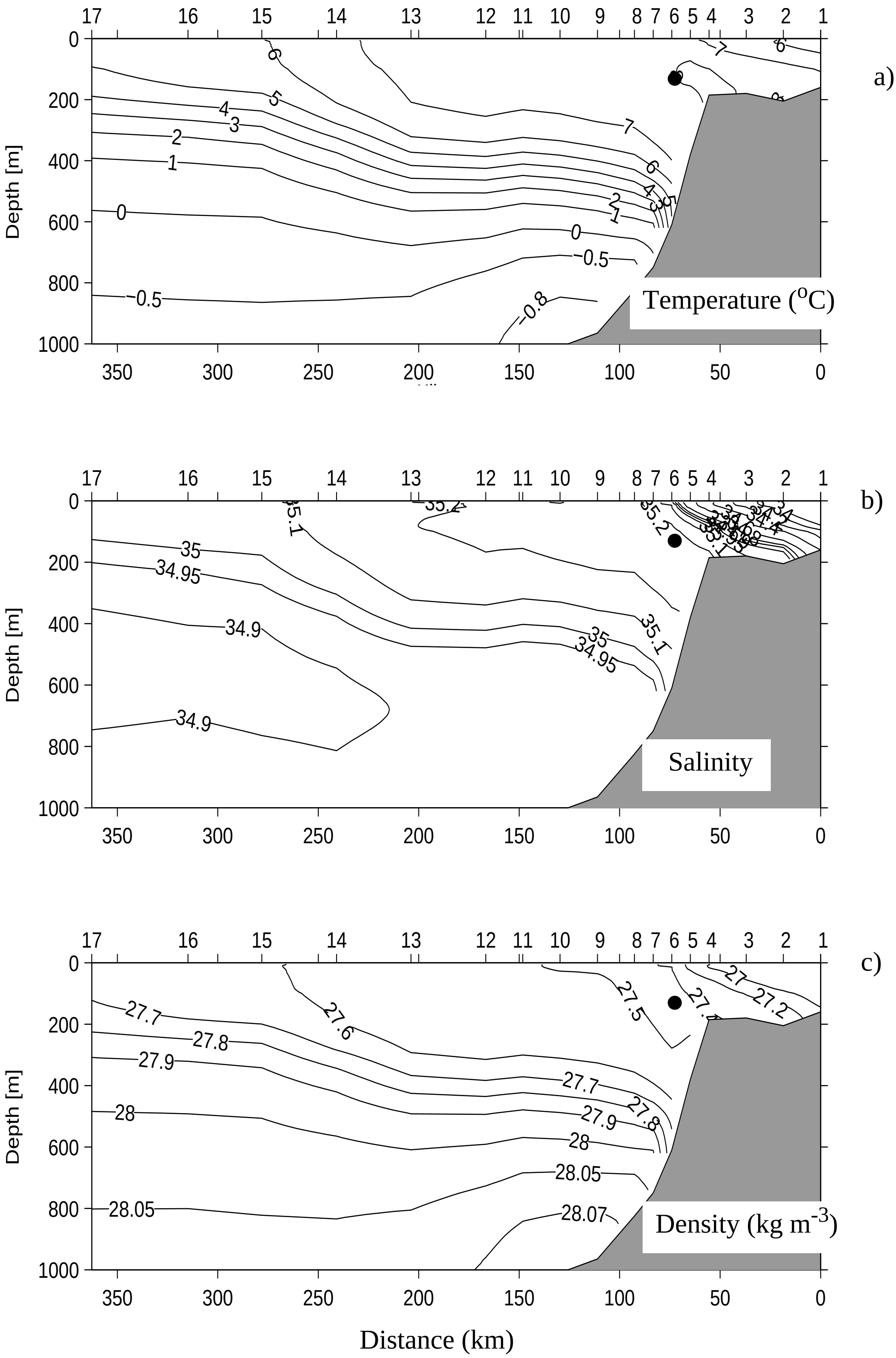
a)
Temperature (°C)
b)
Salinity
c)
Density (kg m-3)
Depth [m]
Distance (km)
17
16
15
14
13
12
11
10
9
8
7
6
5
4
3
2
1
0
200
400
600
800
1000
350
300
250
200
150
100
50
0

Figure 2 a-c

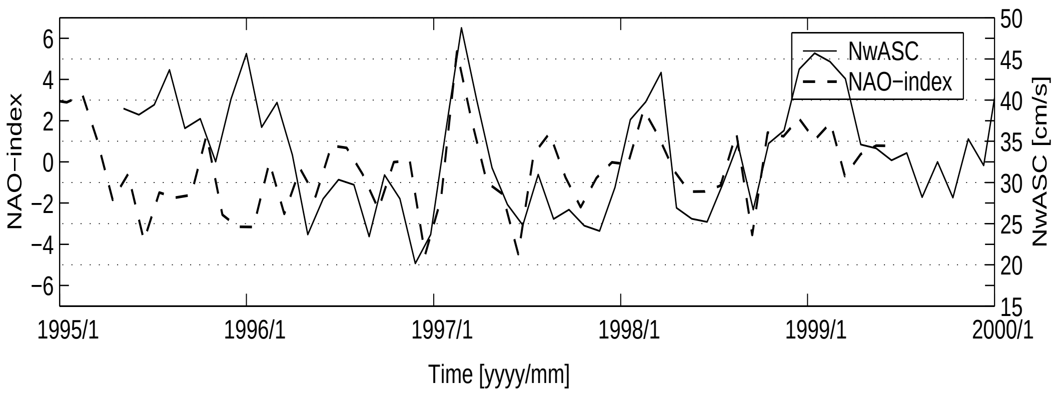

6
4
2
0
−2
−4
−6
NAO−index
50
45
40
35
30
25
20
15
NwASC [cm/s]
1995/1
1996/1
1997/1
1998/1
1999/1
2000/1
Time [yyyy/mm]
NwASC
NAO−index

Figure 3

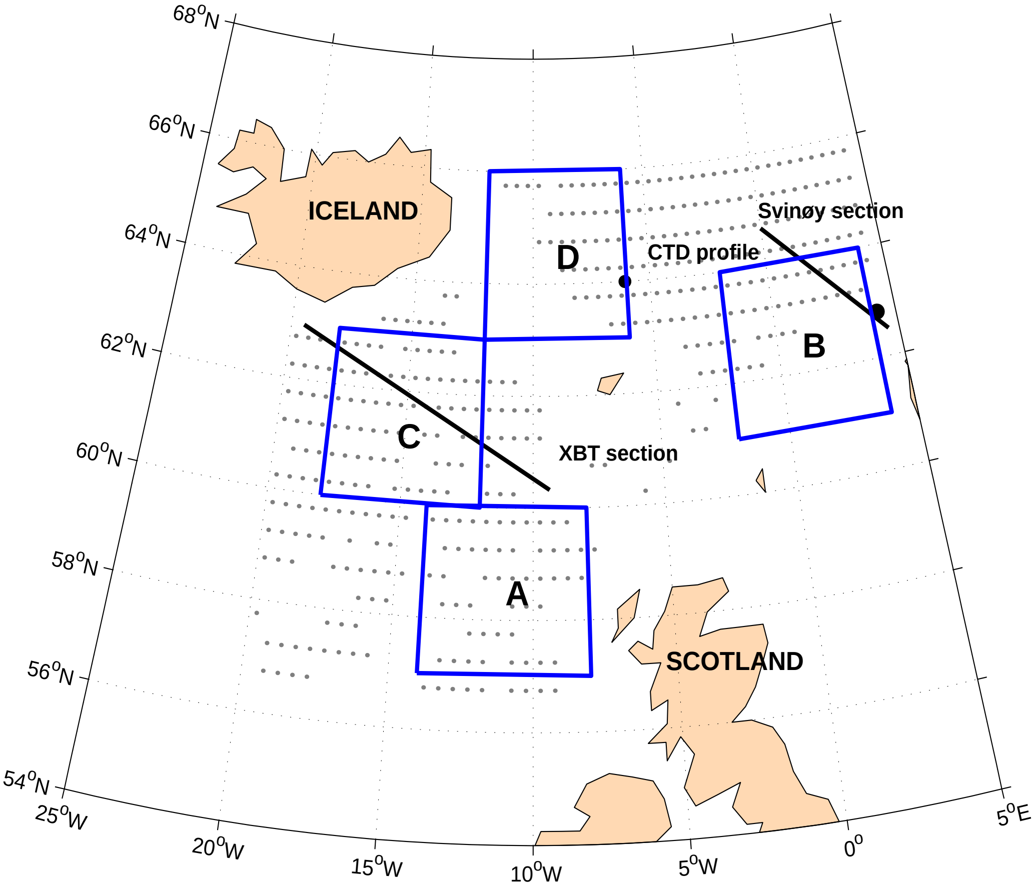

68°N
66°N
64°N
62°N
60°N
58°N
56°N
54°N
25°W
20°W
15°W
10°W
5°W
0°
5°E
ICELAND
SCOTLAND
D
C
A
B
CTD profile
Svinøy section
XBT section

Figure 4

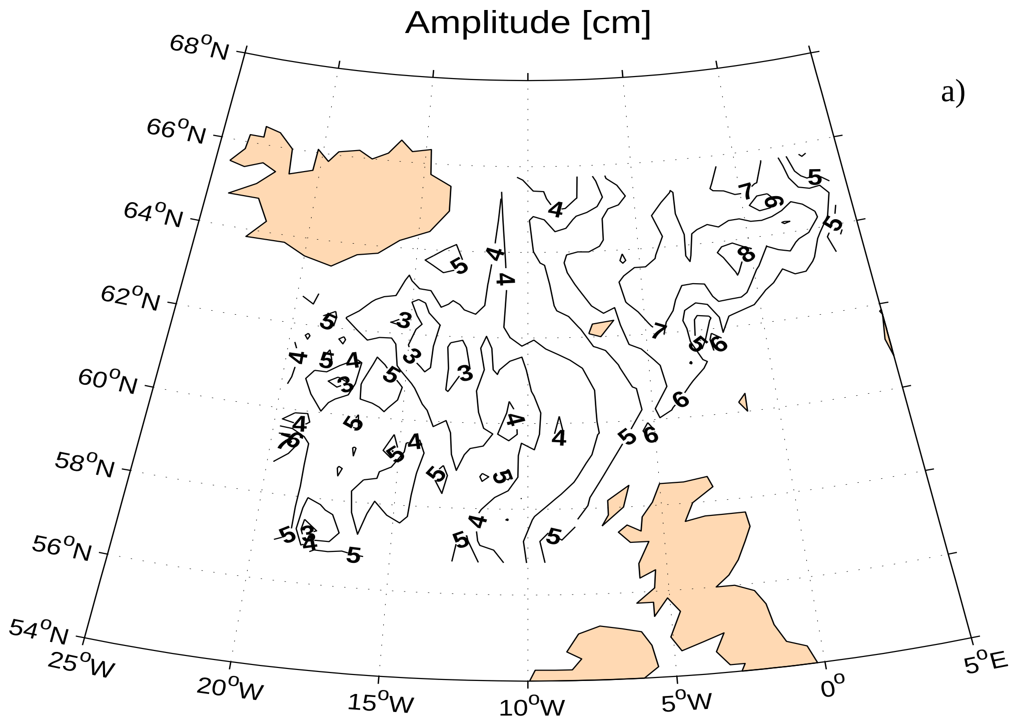
Amplitude [cm]
a)
68°N
66°N
64°N
62°N
60°N
58°N
56°N
54°N
25°W
20°W
15°W
10°W
5°W
0°
5°E

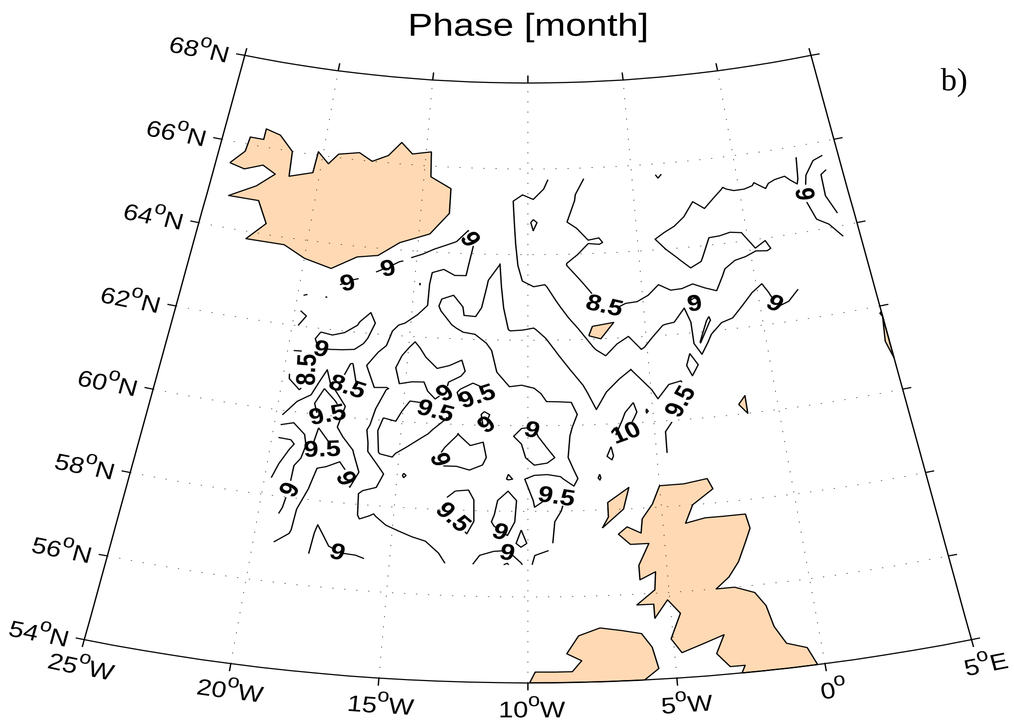
Phase [month]
b)
68°N
66°N
64°N
62°N
60°N
58°N
56°N
54°N
25°W
20°W
15°W
10°W
5°W
0°
5°E

Figure 5 a-c

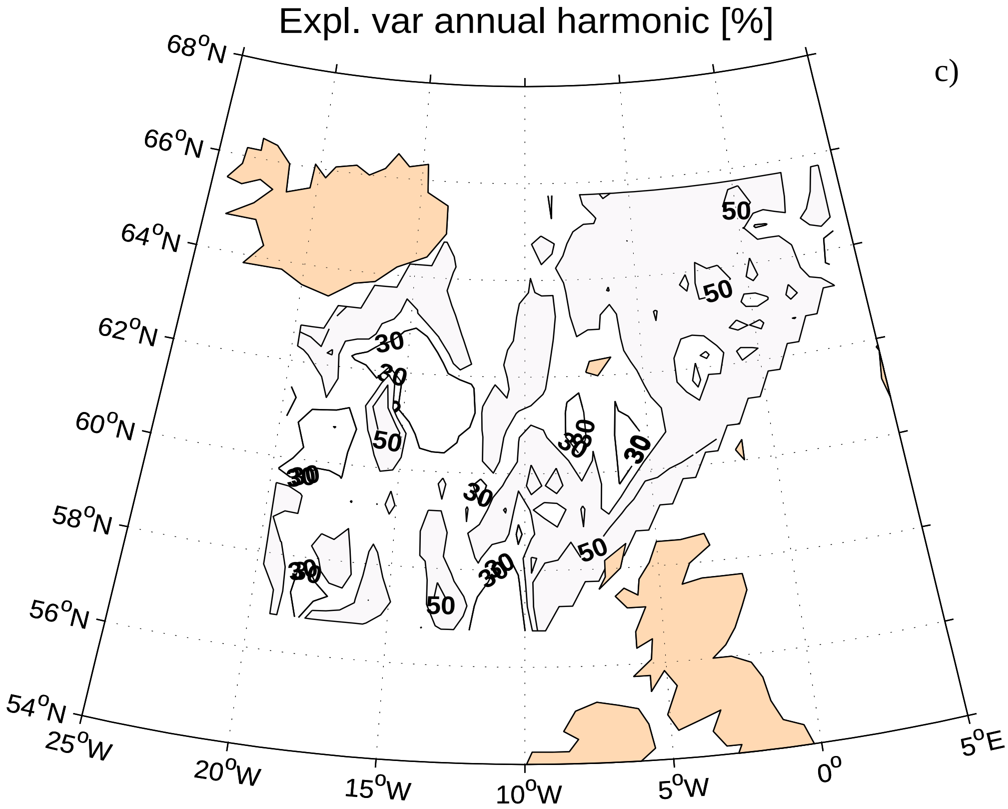

Figure 5 (cont)

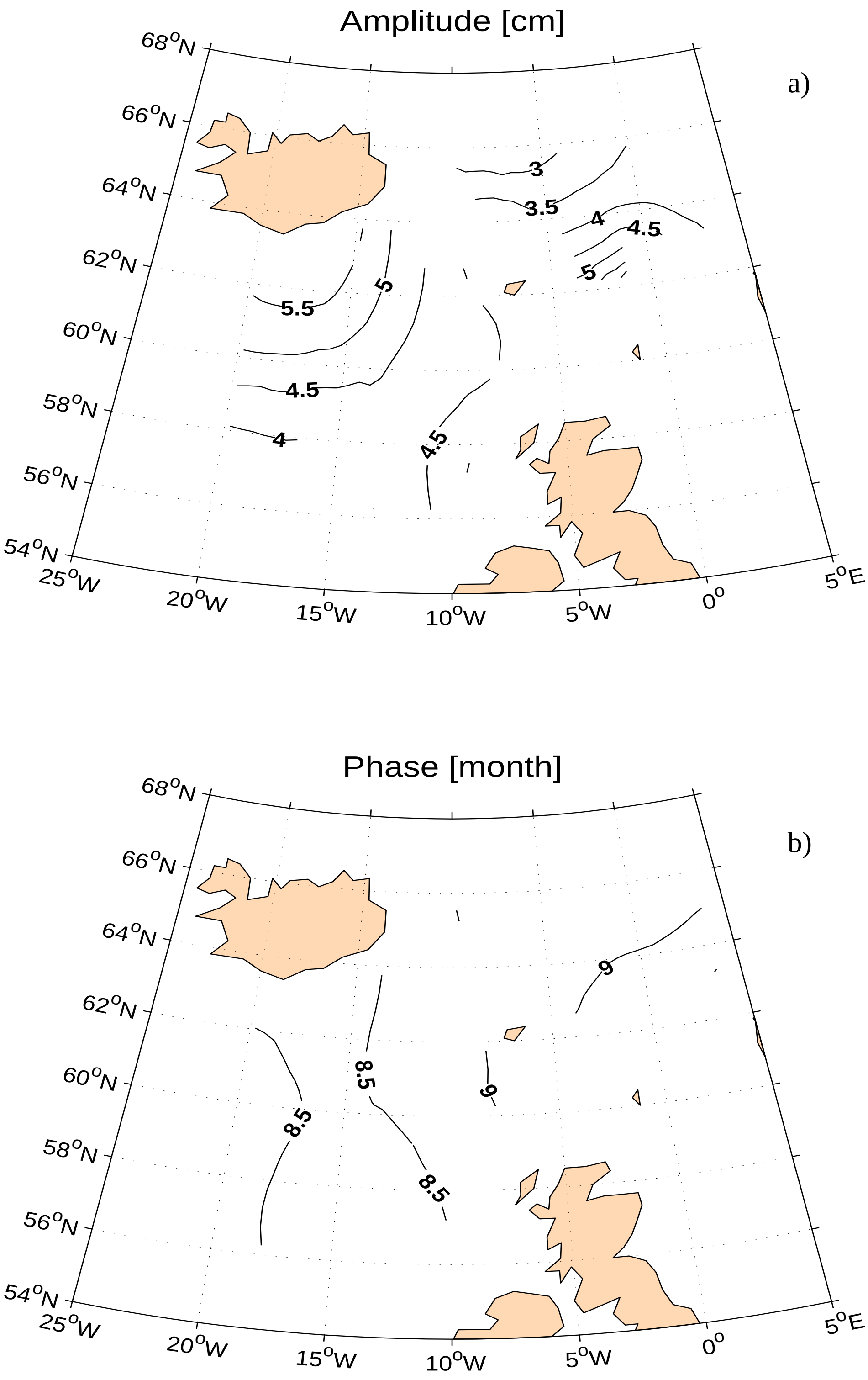
Amplitude [cm]
a)
68°N
66°N
64°N
62°N
60°N
58°N
56°N
54°N
25°W
20°W
15°W
10°W
5°W
0°
5°E
3
3.5
4
4.5
5
5.5
5
4.5
4
4.5
Phase [month]
b)
68°N
66°N
64°N
62°N
60°N
58°N
56°N
54°N
25°W
20°W
15°W
10°W
5°W
0°
5°E
9
8.5
8.5
9
8.5

Figure 6 a-b

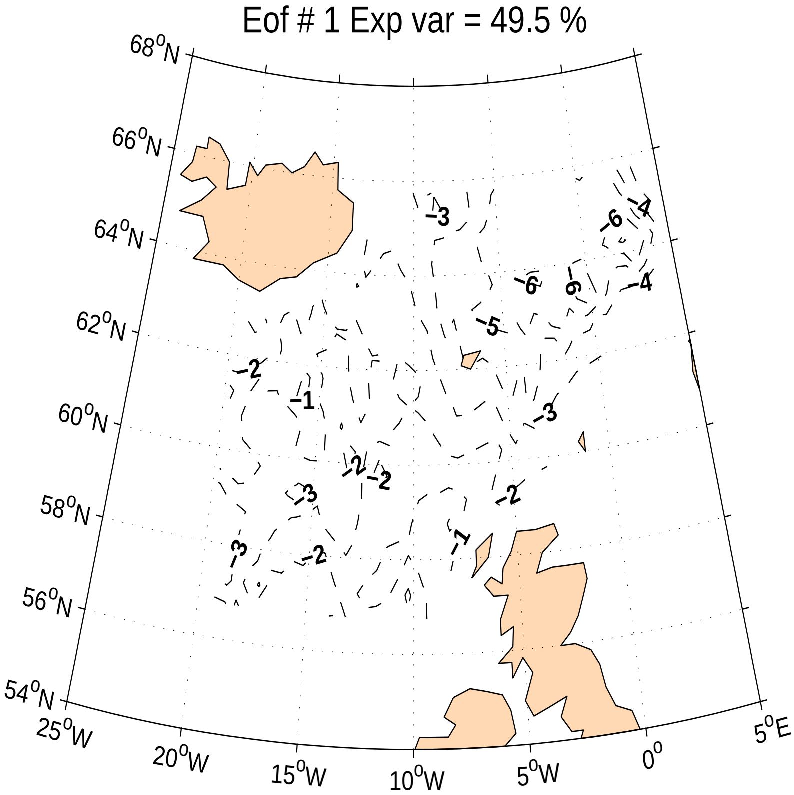

a)

b)

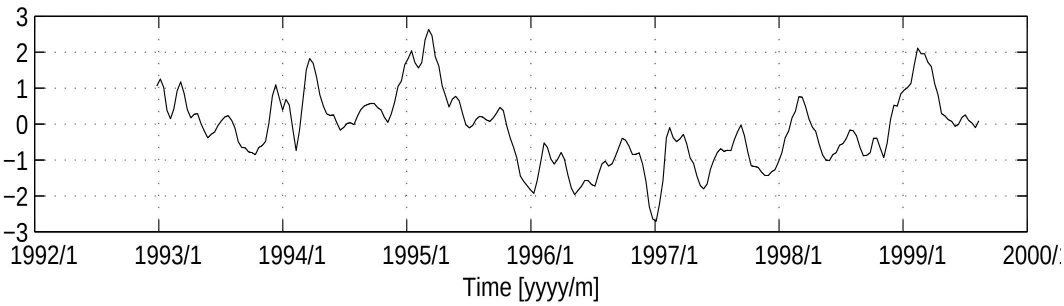

Figure 7 a-d

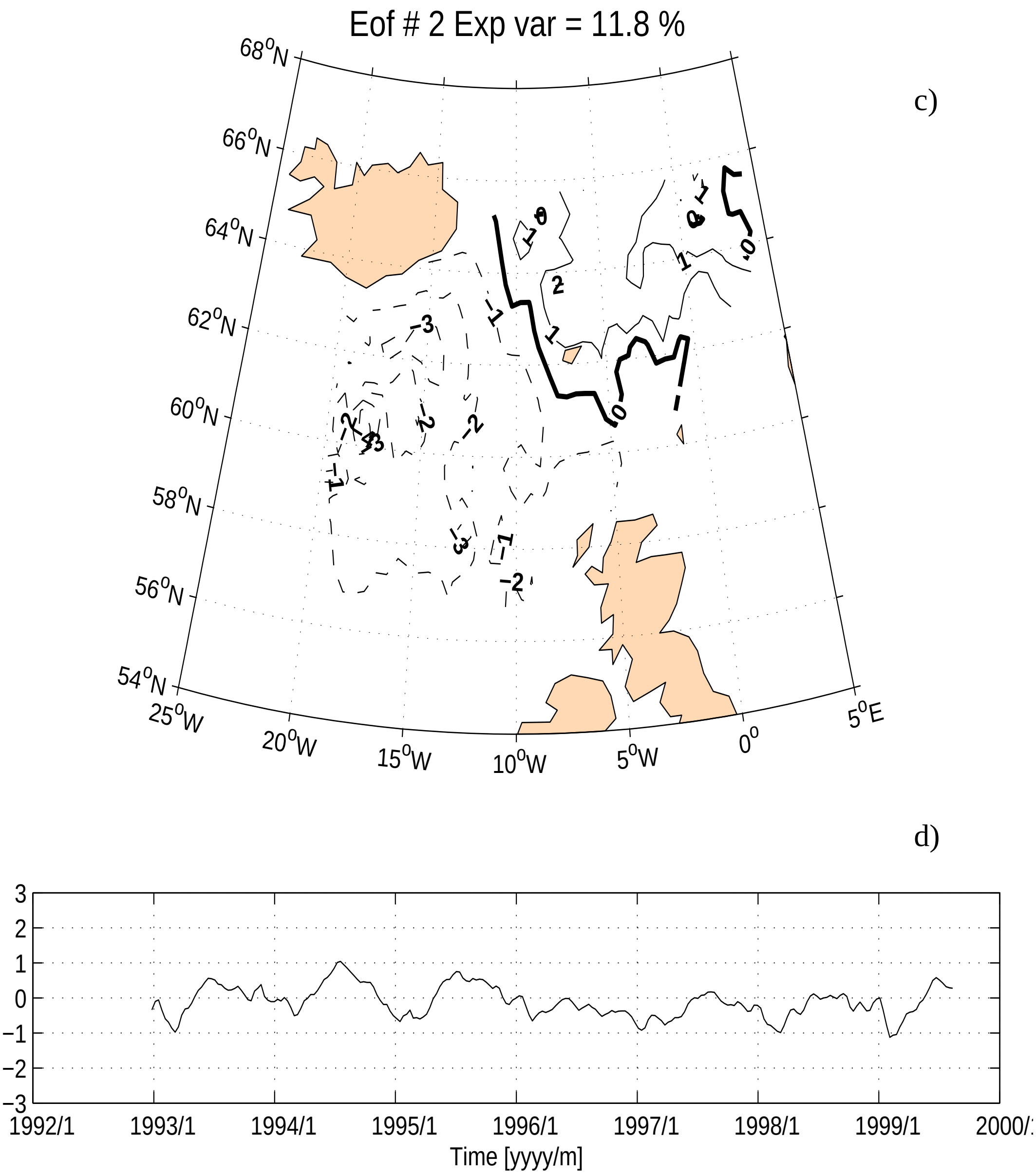

Figure 7 (cont)

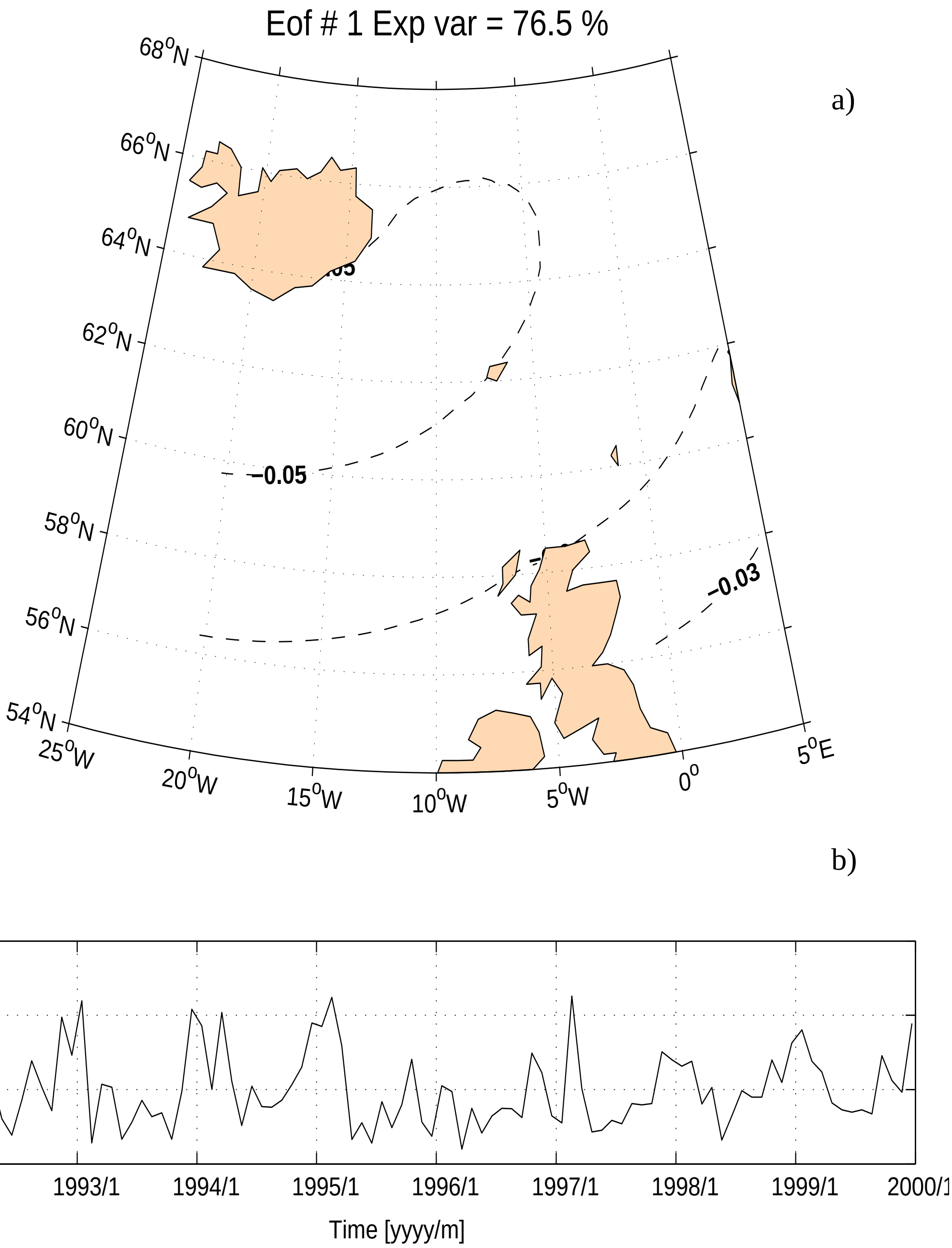

Eof # 1 Exp var = 76.5 %
a)
68°N
66°N
64°N
62°N
60°N
58°N
56°N
54°N
25°W
20°W
15°W
10°W
5°W
0°
5°E
−0.05
−0.03
b)
4
2
0
−2
1992/1
1993/1
1994/1
1995/1
1996/1
1997/1
1998/1
1999/1
2000/1
Time [yyyy/m]

Figure 8 a-b

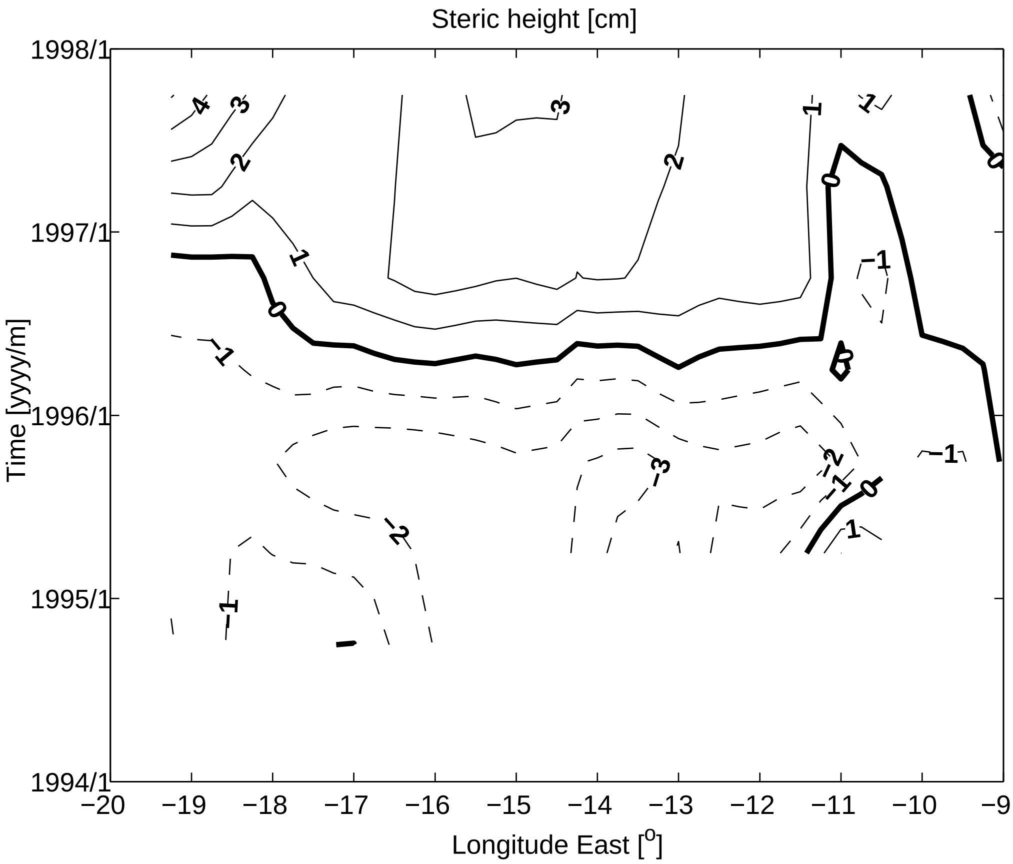

Steric height [cm]
1998/1
1997/1
1996/1
1995/1
1994/1
Time [yyyy/m]
−20
−19
−18
−17
−16
−15
−14
−13
−12
−11
−10
−9
Longitude East [^{0}]

Figure 9

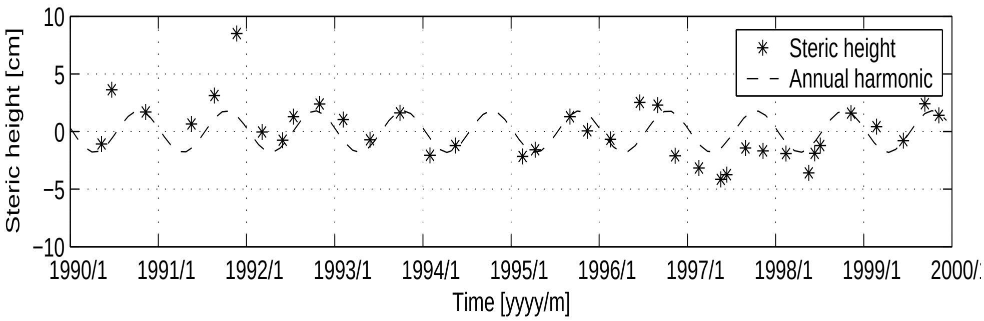
Steric height
Annual harmonic
Steric height [cm]
10
5
0
−5
−10
1990/1
1991/1
1992/1
1993/1
1994/1
1995/1
1996/1
1997/1
1998/1
1999/1
Time [yyyy/m]

Figure 10

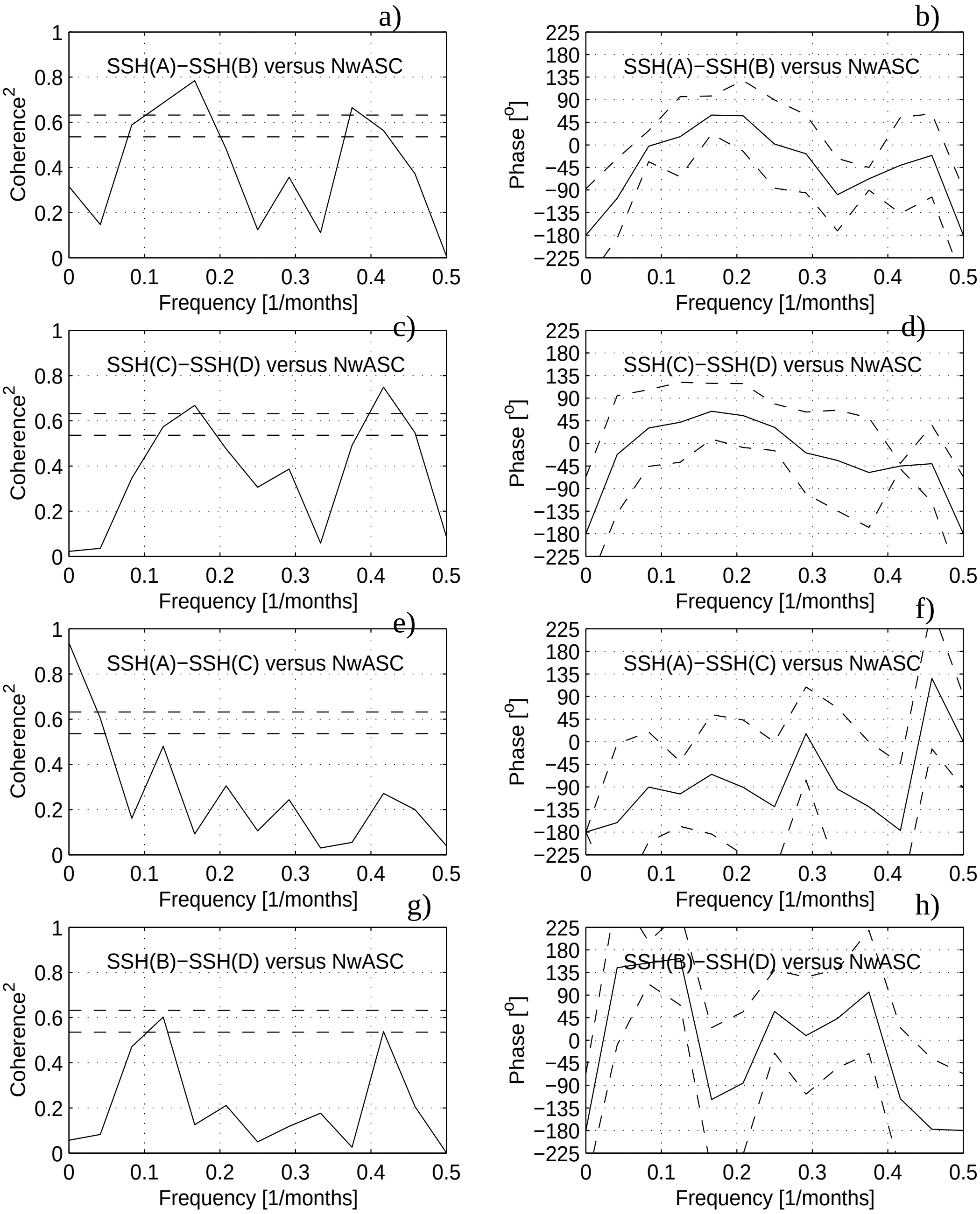
a)
SSH(A)−SSH(B) versus NwASC
b)
SSH(A)−SSH(B) versus NwASC
c)
SSH(C)−SSH(D) versus NwASC
d)
SSH(C)−SSH(D) versus NwASC
e)
SSH(A)−SSH(C) versus NwASC
f)
SSH(A)−SSH(C) versus NwASC
g)
SSH(B)−SSH(D) versus NwASC
h)
SSH(B)−SSH(D) versus NwASC
Coherence^2
Phase [^{o}]
Frequency [1/months]
0
0.1
0.2
0.3
0.4
0.5
0.6
0.8
1
225
180
135
90
45
0
−45
−90
−135
−180
−225

Figure 11 a-h

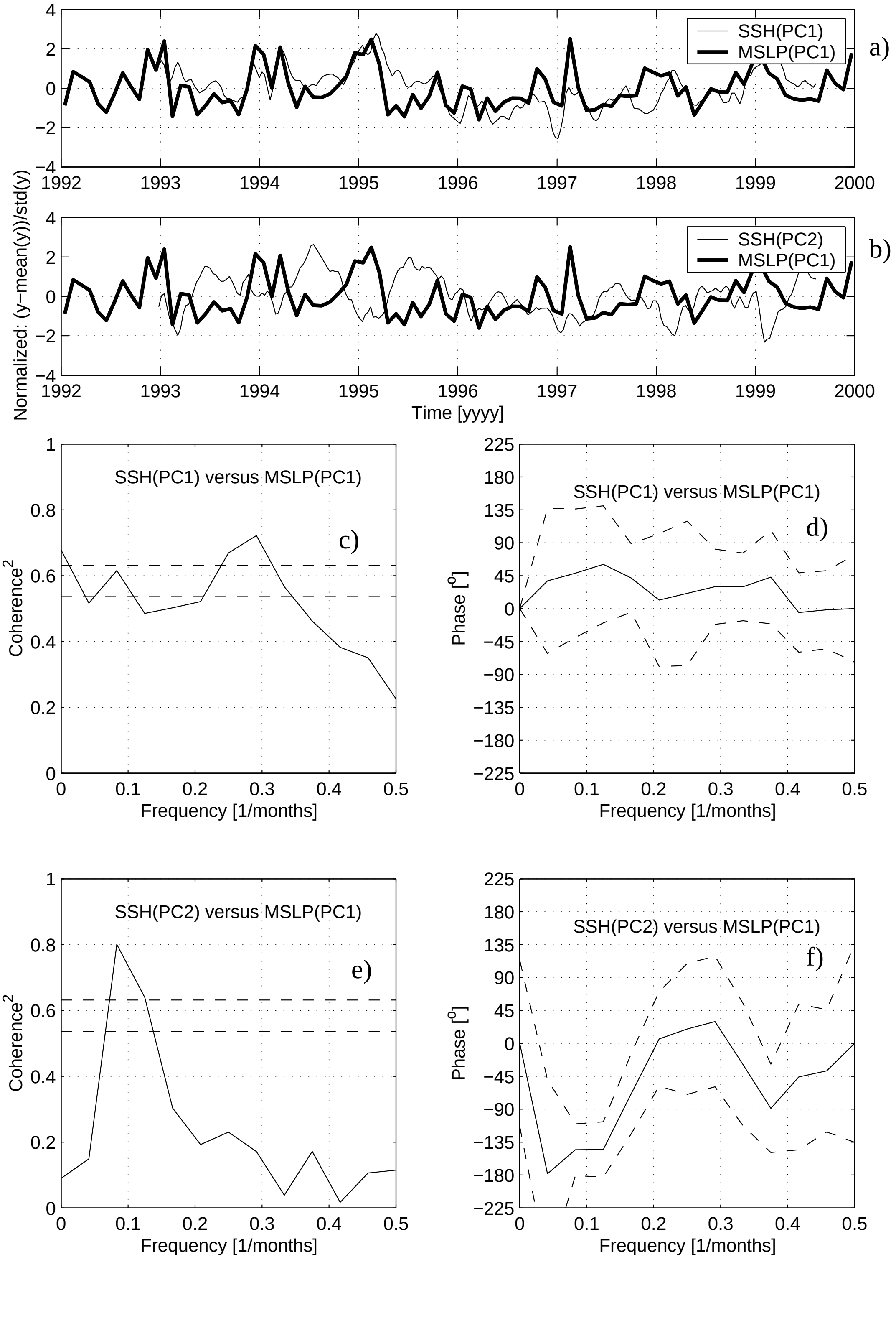
SSH(PC1)
MSLP(PC1)
a)
SSH(PC2)
MSLP(PC1)
b)
Normalized: (y−mean(y))/std(y)
Time [yyyy]
SSH(PC1) versus MSLP(PC1)
c)
SSH(PC1) versus MSLP(PC1)
d)
SSH(PC2) versus MSLP(PC1)
e)
SSH(PC2) versus MSLP(PC1)
f)
Coherence^2
Phase [^{0}]
Frequency [1/months]

Figure 12 a-f

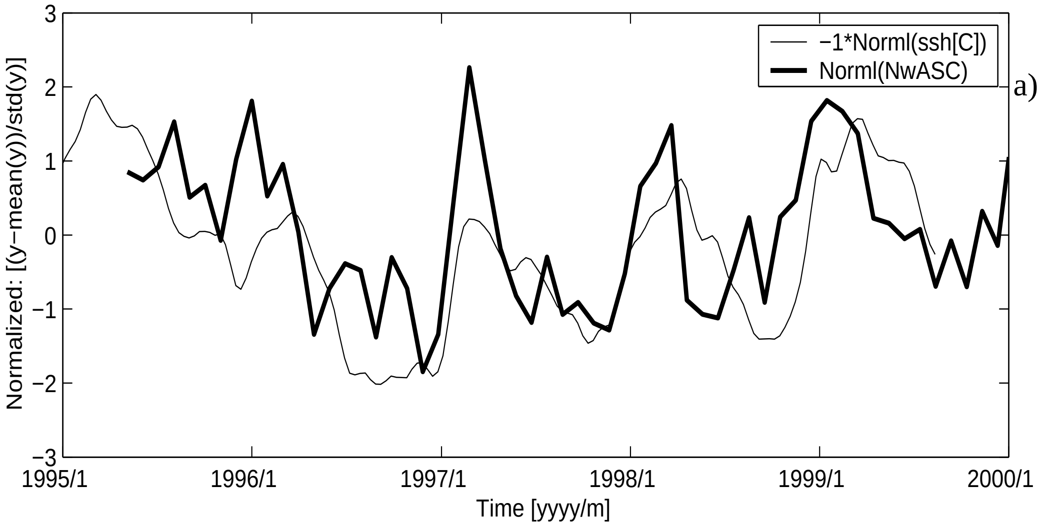
−1*Norml(ssh[C])
Norml(NwASC)
Normalized: [(y−mean(y))/std(y)]
Time [yyyy/m]
1995/1
1996/1
1997/1
1998/1
1999/1
2000/1
3
2
1
0
−1
−2
−3

a)

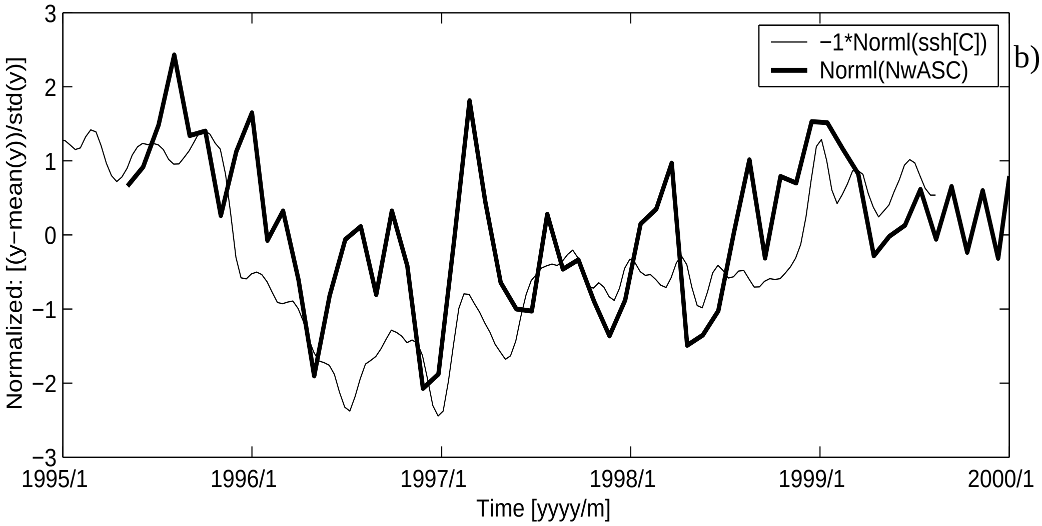
−1*Norml(ssh[C])
Norml(NwASC)
Normalized: [(y−mean(y))/std(y)]
Time [yyyy/m]
1995/1
1996/1
1997/1
1998/1
1999/1
2000/1
3
2
1
0
−1
−2
−3

b)

Figure 13